

# Quinone Oxygen-Coordinated Palladium(II) Complexes with Anthraquinone Ligands Bearing *N*-Heterocyclic Coordination Sites

Toshiyuki Moriuchi,<sup>[a]</sup> Takuo Watanabe,<sup>[a]</sup> Isao Ikeda,<sup>[a]</sup> Akiya Ogawa,<sup>[b]</sup> and Toshikazu Hirao<sup>\*[a]</sup>

**Keywords:** Coordination modes / Quinones / Crystal engineering / Palladium / Redox chemistry

The coordination properties of anthraquinone ligands bearing *N*-heterocyclic coordination sites to divalent palladium, and structural characterization of the quinone oxygen-coordinated palladium(II) complexes are described. The intramolecular NH...O (quinone) hydrogen bond [N(1)...O(2), 2.617 Å] was observed in the crystal structure of 1-chloro-8-[2-(2-pyridyl)ethylamino]-9,10-anthraquinone (**1a**). The anthraquinone moieties of **1a** are oriented in a face-to-face manner to form  $\pi$ -stacks in the crystal, with an interplanar distance of ca. 3.5 Å between the neighboring anthraquinone moieties. Complexation of **1a** with Pd(OAc)<sub>2</sub> afforded the palladium(II) complex **2a**. The quinone oxygen, which is bent out of the anthraquinone plane, is coordinated to the palladium(II) center, which is substituted by the amino nitrogen in a position *trans* to the pyridyl nitrogen in the crystal structure **2a**. 1-(2-Phenylethylamino)-8-[2-(2-pyridyl)ethylamino]-9,10-anthraquinone (**1b**) was also found to form the 1:1 quinone oxygen-coordinated palladium(II) complex **2b**. The single-crystal X-ray structure determination of **2b** shows the existence of two independent molecules in the asymmetric unit. These two molecules are present in a good mirror image

relationship, indicating conformational enantiomers. Furthermore, they are overlapped in a face-to-face manner to form the  $\pi$ -stack dimer, which arranges in a herringbone motif with the virtues of offset stacking and edge-to-face contacts in the crystal packing. Starting from 1,5-bis[2-(2-pyridyl)ethylamino]-9,10-anthraquinone (**1c**) bearing two *N*-heterocyclic coordination sites, the conjugated palladium(II) homobimetallic complex **2c** was obtained. Two palladium atoms are bridged by the quinone moiety to afford a redox-active conjugated homobimetallic complex system. The crystal structure of **2c** reveals that two palladium atoms are disposed on opposite faces of the anthraquinone plane, accompanied by the bend of the quinone oxygens out of the anthraquinone plane. The anthraquinone moieties of **2c** are arranged in an edge-to-face orientation in the crystal packing. In the palladium(II) complexes **2b–c**, the d, $\pi$ -conjugated system is interconnected through a  $\pi$ - $\pi$  interaction between the  $\pi$ -conjugated systems. The cyclic voltammograms of these quinone oxygen-coordinated palladium(II) complexes **2a–c** show two redox couples based on the quinone moiety, which are positively shifted relative to the free quinone ligands.

## Introduction

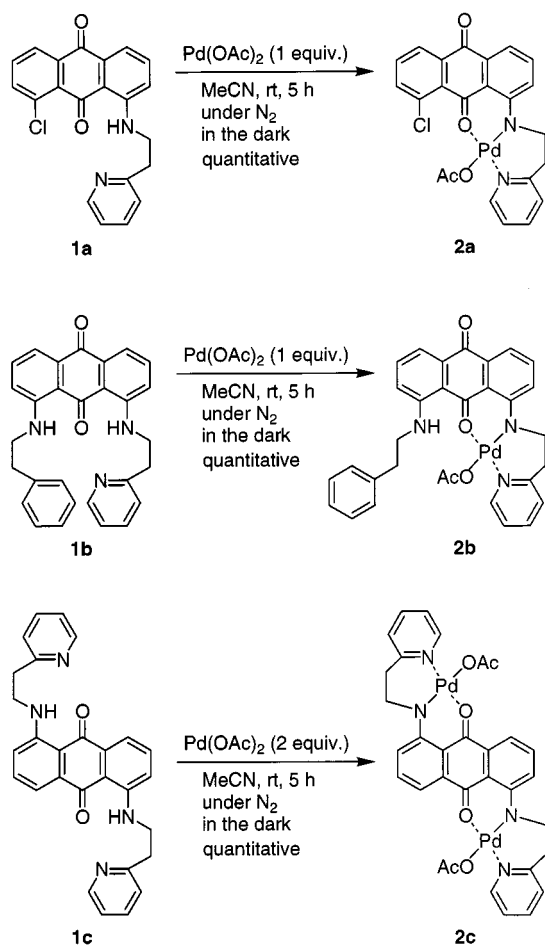
Efficient redox processes of transition metal complexes are one of the key factors in developing versatile systems for new materials and catalytic redox reactions. Since ligand coordination greatly contributes to redox processes, ligand design is often crucial for the construction of an efficient redox system. From this point of view, the redox-active quinone ligands, which are present in three redox forms (the reduced hydroquinone dianions, the partially reduced semiquinone radical anions, and the oxidized neutral quinones) are considered to permit an efficient redox system. A variety of transition metal complexes with *o*-quinones or their reduced forms have been prepared and studied extensively.<sup>[1]</sup> For *p*-quinone ligands, Bäckvall has demonstrated the involvement of the  $\pi$ -coordination of *p*-quinone to a Pd<sup>0</sup> center in the Pd-catalyzed oxidation of olefins and conjugated dienes.<sup>[2]</sup> The redox properties of the Pd<sup>0</sup> complexes

with  $\pi$ -bound *p*-quinone ligands have also been investigated.<sup>[3]</sup> However, the *p*-quinone complexes, in which a quinone oxygen coordinates to a high valent transition metal, have not been investigated extensively,<sup>[4]</sup> despite the elucidation of their coordination and redox properties in catalysis. In our previous papers,<sup>[5]</sup> the  $\pi$ -conjugated molecule, *N,N'*-bis(4'-dimethylaminophenyl)-1,4-benzoquinone diimine, was introduced to the palladium(II) complex bearing the *N*-heterocyclic tridentate podand ligand, affording a redox-active  $\pi$ -conjugated palladium(II) homobimetallic complex, in which the redox properties of the quinone diimine moiety are modulated by complexation. These results prompted us to investigate the redox properties of the transition metal complexes with *p*-quinones and to characterize the complexes structurally. Another interesting feature depends on the  $\pi$ - $\pi$  interactions between the anthraquinone aromatic rings in the crystal packing.<sup>[6]</sup> This interaction could induce architecturally controlled self-assembly, leading to molecular aggregates in the solid state. The  $\pi$ - $\pi$  interaction between the  $\pi$ -conjugated moieties of the conjugated complexes is considered to be one of the most convenient approaches for the assembly of the conjugated complexes. In this context, we herein report the coordination properties of anthraquinone ligands bearing *N*-heterocyclic coordination sites to

<sup>[a]</sup> Department of Applied Chemistry, Faculty of Engineering, Osaka University, Yamada-oka, Suita, Osaka 565–0871, Japan  
E-mail: hirao@ap.chem.eng.osaka-u.ac.jp

<sup>[b]</sup> Department of Chemistry, Faculty of Science, Nara Women's University, Kita-uoyanishi-machi, Nara 630–8506, Japan

divalent palladium, and the structural characterization of the quinone oxygen-coordinated palladium(II) complexes.



Scheme 1

## Results and Discussion

The anthraquinone ligands **1a–c** were prepared from the corresponding chloroanthraquinones and 2-(2-aminoethyl)-pyridine (Scheme 1). These anthraquinone ligands were fully characterized by spectroscopic techniques and elemental analysis. The FT-IR spectra of the anthraquinone ligands **1a–c** show hydrogen-bonded NH and C=O stretching bands (**1a**: 3286 and 1635 cm<sup>-1</sup>, **1b**: 3263 and 1620 cm<sup>-1</sup>, **1c**: 3255 and 1620 cm<sup>-1</sup>, Table 1). The crystal structure of **1a** supports the presence of an intramolecular hydrogen bond between NH and C=O (quinone) [N(1)⋯O(2), 2.617 Å; H⋯O(2), 1.88 Å, Figure 1 and Table 2], indicating a slightly longer carbonyl bond [O(2)–C(13), 1.224 Å] than the non-hydrogen bonded carbonyl bond [O(1)–C(6), 1.216 Å]. Selected bond lengths and bond angles are listed in Table 3. It is notable that the anthraquinone moieties of **1a** are oriented in a face-to-face

Table 1. Selected spectroscopic data

	FT-IR		E <sub>1/2</sub> (V) <sup>[a]</sup>	
	ν <sub>N-H</sub> (cm <sup>-1</sup> )	ν <sub>C=O</sub> (cm <sup>-1</sup> )	q/sq	sq/hq
<b>1a</b>	3286	1658, 1635	-1.44	-1.94
<b>2a</b>	—	1651, 1620	-1.32	-1.73
<b>1b</b>	3263	1658, 1620	-1.56	-1.98
<b>2b</b>	3332	1643, 1620	-1.40	-1.81
<b>1c</b>	3255	1620	-1.57	-1.87
<b>2c</b>	—	1620	-1.31	-1.61

[a] V vs. Fc/Fc<sup>+</sup>.

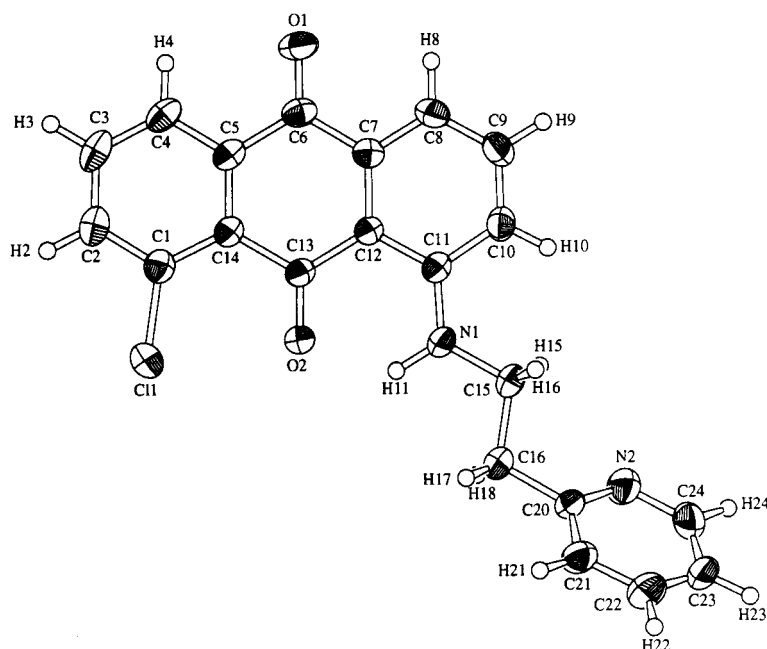


Figure 1. Molecular structure of **1a** (40% probability ellipsoids)

manner with an interplanar distance of ca. 3.5 Å between the neighboring anthraquinone moieties, which form  $\pi$ -stacks in the crystal as shown in Figure 2. The arrangement of  $\pi$ -stacks represents an offset  $\pi$ -stacked geometry which places one carbonyl oxygen atom directly above the carbonyl carbon atom of the neighboring molecule.

Complexation of **1a** with Pd(OAc)<sub>2</sub> in acetonitrile afforded the 1:1 palladium(II) complex **2a** (Scheme 1). The formation of **2a** was followed by spectrophotometric titration. Thus, the absorption around 647 nm due to **2a** appeared and increased until the ratio of [1a]/[Pd(OAc)<sub>2</sub>] was 1:1, with concomitant disappearance of the absorption of

Table 2. Crystallographic data for **1a**, **2a**, **2b**, and **2c**

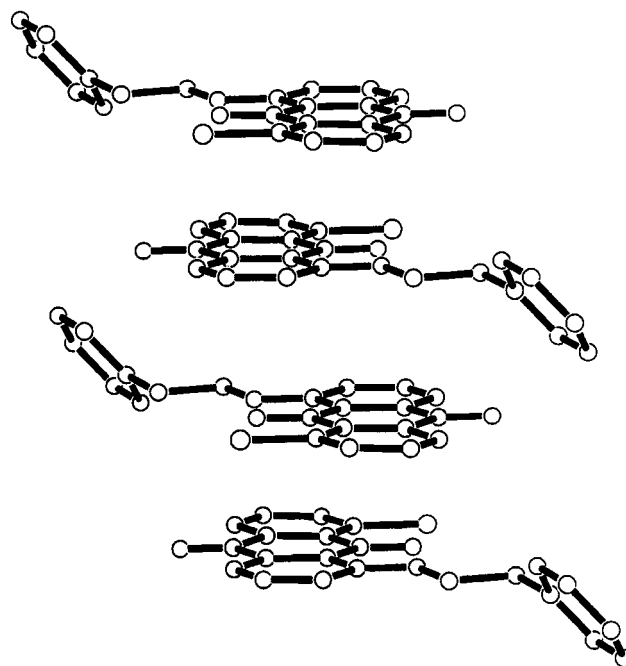
	<b>1a</b>	<b>2a</b>	<b>2b</b>	<b>2c</b>
Empirical formula	C <sub>21</sub> H <sub>15</sub> N <sub>2</sub> O <sub>2</sub> Cl	C <sub>23</sub> H <sub>17</sub> N <sub>2</sub> O <sub>4</sub> ClPd · H <sub>2</sub> O	C <sub>31</sub> H <sub>27</sub> N <sub>3</sub> O <sub>4</sub> Pd	C <sub>32</sub> H <sub>28</sub> N <sub>4</sub> O <sub>6</sub> Pd <sub>2</sub> · CH <sub>3</sub> CN
Formula weight	362.81	545.27	611.97	818.45
Crystal system	monoclinic	monoclinic	triclinic	triclinic
Space group	<i>P</i> 2 <sub>1</sub> /n (No. 14)	<i>P</i> 2 <sub>1</sub> /c (No. 14)	<i>P</i> 1̄ (No. 2)	<i>P</i> 1̄ (No. 2)
<i>a</i> [Å]	7.054(3)	10.212(9)	16.822(4)	16.895(3)
<i>b</i> [Å]	10.605(3)	8.004(4)	14.750(3)	16.932(4)
<i>c</i> [Å]	22.582(2)	26.005(3)	11.021(3)	14.441(4)
$\alpha$ [°]			89.99(2)	112.54(2)
$\beta$ [°]	94.02(2)	93.91(2)	108.77(2)	111.65(2)
$\gamma$ [°]			90.00(2)	62.44(2)
<i>V</i> [Å <sup>3</sup> ]	1685.0(7)	2120(1)	2588(1)	3288(1)
<i>Z</i>	4	4	4	4
<i>D</i> <sub>calcd</sub> [g cm <sup>-3</sup> ]	1.430	1.708	1.570	1.653
$\mu$ (Mo K $\alpha$ ) [cm <sup>-1</sup> ]	2.45	10.41	7.61	11.47
<i>T</i> [°C]	23	23	23	23
$\lambda$ (Mo K $\alpha$ ) [Å]	0.71069	0.71069	0.71069	0.71069
<i>R</i> <sup>[a]</sup>	0.062	0.042	0.059	0.058
<i>R</i> <sub>w</sub> <sup>[b]</sup>	0.101	0.031	0.063	0.069

[a]  $R = \sum ||F_o| - |F_c|| / \sum |F_o|$ . [b]  $R_w = [\sum w(|F_o| - |F_c|)^2 / \sum w F_o^2]^{1/2}$ .

Table 3. Selected bond lengths [Å] and bond angles [°] for **1a**, **2a**, and **2b**

	1a	2a	2b <sup>[a]</sup>	
Bond lengths				
Pd–O(2)	----	1.970(3)	1.985(7)	1.987(7)
Pd–O(3)	----	2.031(3)	2.058(8)	2.056(8)
Pd–N(1)	----	1.974(3)	1.994(8)	1.985(8)
Pd–N(2)	----	2.010(4)	2.026(9)	2.015(9)
O(1)–C(6)	1.216(7)	1.217(6)	1.24(1)	1.23(1)
O(2)–C(13)	1.224(6)	1.266(5)	1.28(1)	1.28(1)
N(1)–C(11)	1.365(7)	1.327(5)	1.32(1)	1.34(1)
C(10)–C(11)	1.421(8)	1.447(6)	1.40(1)	1.42(1)
C(11)–C(12)	1.424(7)	1.457(6)	1.45(1)	1.42(1)
C(12)–C(13)	1.474(8)	1.414(6)	1.44(1)	1.42(1)
C(13)–C(14)	1.508(7)	1.502(6)	1.48(1)	1.49(1)
Bond angles				
O(2)–Pd–O(3)	----	85.5(1)	91.1(3)	91.0(3)
O(2)–Pd–N(1)	----	90.8(1)	88.4(3)	88.4(3)
O(3)–Pd–N(2)	----	89.3(2)	85.8(4)	86.1(4)
N(1)–Pd–N(2)	----	94.4(2)	94.5(3)	94.4(4)
O(2)–Pd–N(2)	----	172.5(2)	175.6(3)	175.8(3)
O(3)–Pd–N(1)	----	176.3(1)	175.7(4)	176.0(4)
C(13)–O(2)–Pd	----	127.6(3)	129.4(7)	128.4(7)
C(11)–N(1)–Pd	----	124.1(3)	124.7(7)	124.1(7)
O(2)–C(13)–C(14)	119.6(5)	113.7(4)	115.0(10)	113.4(10)
O(2)–C(13)–C(12)	121.5(5)	125.2(4)	122.7(9)	123.9(10)
C(11)–C(12)–C(13)	120.5(5)	122.4(4)	123.2(9)	123.1(10)
C(12)–C(11)–N(1)	122.2(5)	124.9(4)	124.2(9)	124.6(10)
C(10)–C(11)–N(1)	120.0(5)	119.7(4)	119.6(10)	119.0(10)
C(11)–N(1)–C(15)	123.1(5)	117.4(4)	116.6(9)	116.9(9)

[a] Two independent molecules exist in the asymmetric unit.

Figure 2. Crystal packing diagram of **1a** showing extended  $\pi$ -stacking

**1a** around 505 nm (Figure 3). This result supports the formation of the 1:1 complex **2a**. The structure of the isolated complex **2a** was elucidated by <sup>1</sup>H NMR spectroscopy. The absence of an amine proton in the <sup>1</sup>H NMR spectrum indicates the displacement of the acetate ligands of Pd(OAc)<sub>2</sub> by the amino nitrogen of **1a**. The down-field shift

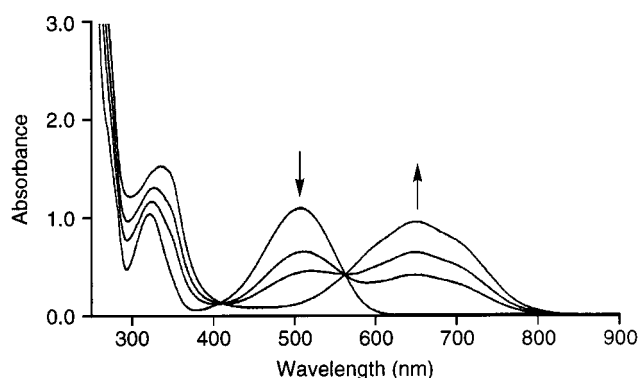


Figure 3. UV/Vis spectra on successive treatment of **1a** ( $1.0 \times 10^{-4}$  M) with  $\text{Pd}(\text{OAc})_2$  (0, 0.4, 0.6,  $1.0 \times 10^{-4}$  M) in MeCN under argon

of the pyridyl protons implies the coordination of the pyridyl nitrogen to palladium.

Further structural information for **2a** was obtained by an X-ray crystal structure determination (Figure 4 and Table 2). The quinone oxygen and pyridyl nitrogen atoms coordinate to palladium in a *trans* fashion. The coordinated quinone carbonyl bond [ $\text{O}(2)-\text{C}(13)$ , 1.266 Å] is longer than the uncoordinated one [ $\text{O}(1)-\text{C}(6)$ , 1.217 Å], which is consistent with the observation of two kinds of  $\text{C}=\text{O}$  stretching bands ( $1651$  and  $1620\text{ cm}^{-1}$ ) in the FT-IR spectrum of **2a**. The bond lengths of both  $\text{N}(1)-\text{C}(11)$  and  $\text{C}(12)-\text{C}(13)$  are shortened upon complexation [**1a**:  $\text{N}(1)-\text{C}(11)$ , 1.365 Å;  $\text{C}(12)-\text{C}(13)$ , 1.474 Å; **2a**:  $\text{N}(1)-\text{C}(11)$ , 1.327 Å;  $\text{C}(12)-\text{C}(13)$ , 1.414 Å]. The  $\text{O}(2)-\text{C}(13)-\text{C}(12)$  and  $\text{C}(12)-\text{C}(11)-\text{N}(1)$  angles increase slightly to accommodate the palladium atom [**1a**:  $\text{O}(2)-\text{C}(13)-\text{C}(12)$ ,  $121.5^\circ$ ;  $\text{C}(12)-\text{C}(11)-\text{N}(1)$ ,  $122.2^\circ$ ; **2a**:  $\text{O}(2)-\text{C}(13)-\text{C}(12)$ ,  $125.2^\circ$ ;  $\text{C}(12)-\text{C}(11)-\text{N}(1)$ ,  $124.9^\circ$ ]. Additionally, the palladium center deviates considerably from the anthraquinone plane. The coordination

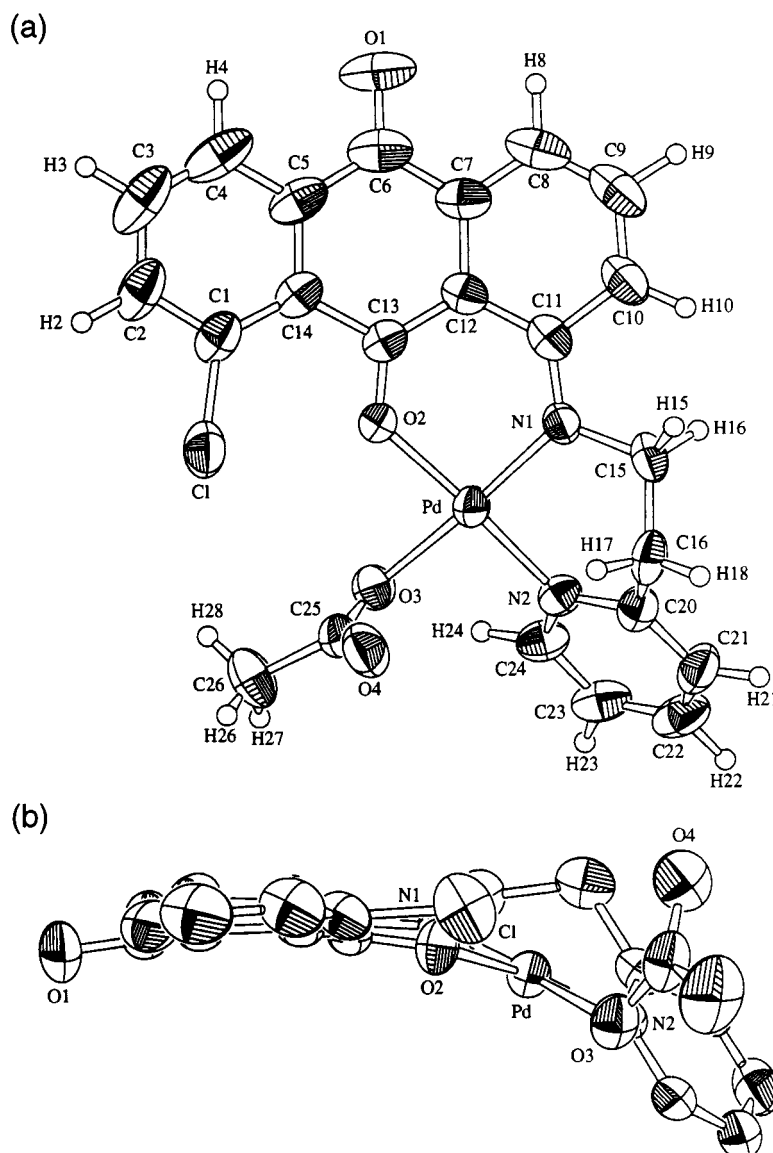


Figure 4. (a) Top view and (b) side view of the molecular structure of **2a** (40% probability ellipsoids. Hydrogen atoms are omitted for clarity)

geometry is almost square planar with the palladium-bonded amino nitrogen in a position *trans* to the acetoxy group. Another interesting feature lies in the nonplanar anthraquinone skeleton of **2a**, which is in sharp contrast to the planar one of **1a**. The two phenyl rings in the anthraquinone moiety form a V shape intersecting at C(6) and C(13) with a dihedral angle of  $15.2^\circ$ , where O(1) and O(2) are bent slightly out of the anthraquinone plane, as shown in Figure 4b. The  $\pi$ -stacks observed for **1a** are not observed in the crystal packing of **2a**, possibly due to the nonplanar anthraquinone skeleton (Figure 5).

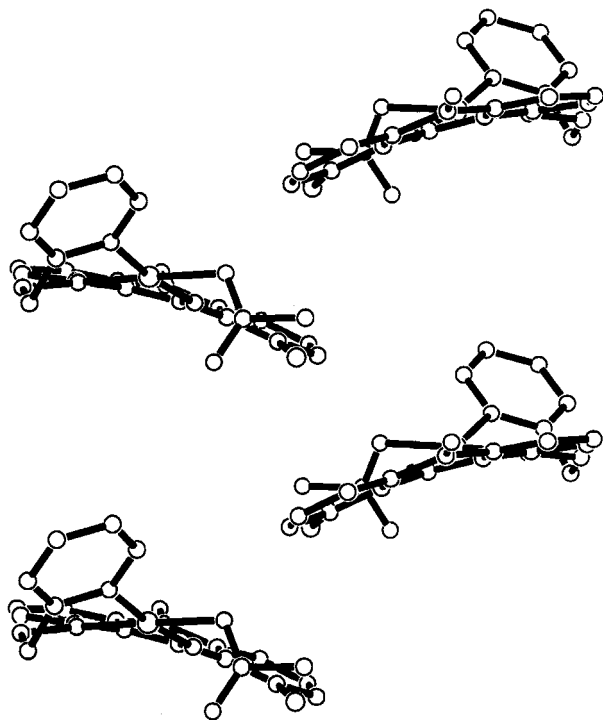


Figure 5. Crystal packing diagram obtained for **2a**

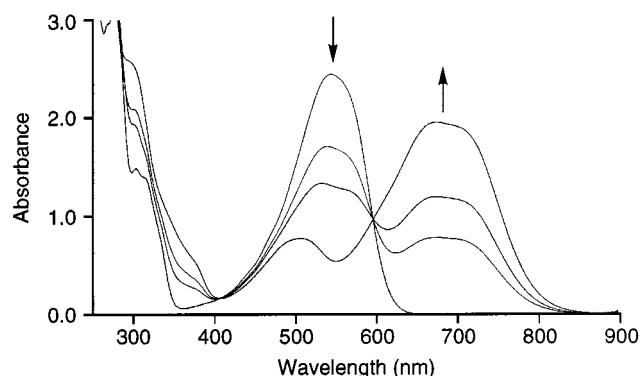


Figure 6. UV/Vis spectra on successive treatment of **1b** ( $1.0 \times 10^{-4}$  M) with  $\text{Pd}(\text{OAc})_2$  (0, 0.4, 0.6,  $1.0 \times 10^{-4}$  M) in MeCN under argon

On the basis of these observations, the complexation behavior and molecular arrangement of the unsymmetrical anthraquinone ligand **1b** was studied to gain insight into the effect of the pendant group at the 8-position. Treatment of **1b** with  $\text{Pd}(\text{OAc})_2$  in acetonitrile afforded the 1:1 complex **2b** (Scheme 1). A similar spectral change was observed to support the formation of the palladium(II) complex **2b**, which exhibited a broad band around 675 nm (Figure 6). In the  $^1\text{H}$  NMR spectrum of the isolated complex **2b**, the down-field shift of the pyridyl protons, and no shift of the phenylethyl group indicate that the nitrogen of the phenylethylamino group does not coordinate.

The crystal structure of **2b** is also characterized by a quinone oxygen-coordinated square planar geometry, in which the palladium atom is deviated from the anthraquinone plane, as observed in **2a** (Figure 7 and Table 2). As **2b** crystallized in the space group  $P\bar{1}$  with  $Z = 4$ , two independent molecules exist in the asymmetric unit. Noteworthy, they are present in a good mirror image relationship as depicted in Figure 8. However, the barrier of interconversion of these

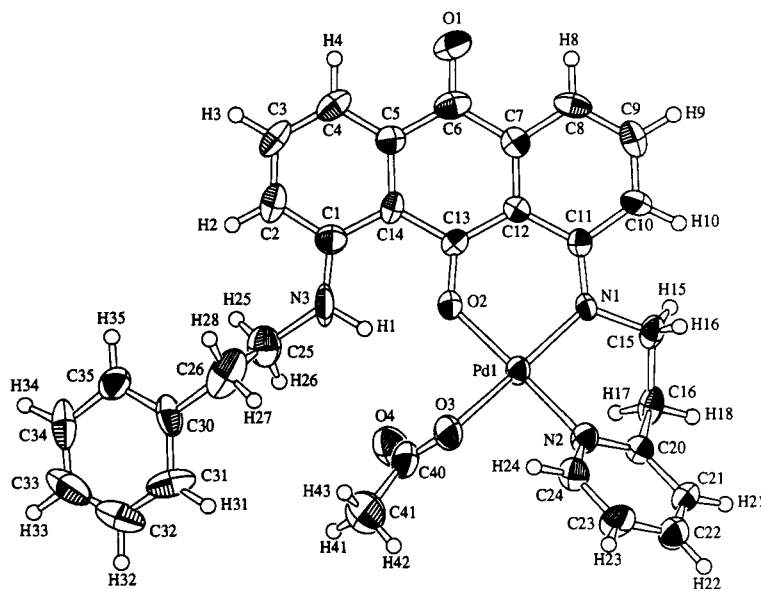


Figure 7. Molecular structure of **2b** (40% probability ellipsoids)

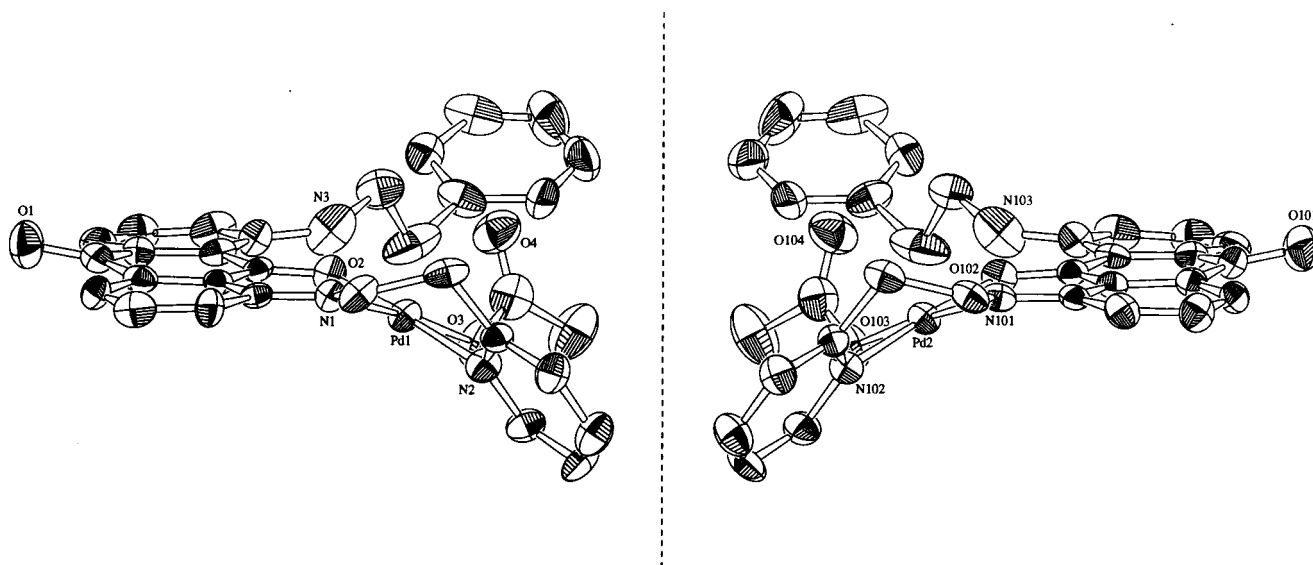


Figure 8. Conformational enantiomers of **2b** (40% probability ellipsoids); the enantiomorphs are related by the mirror plane

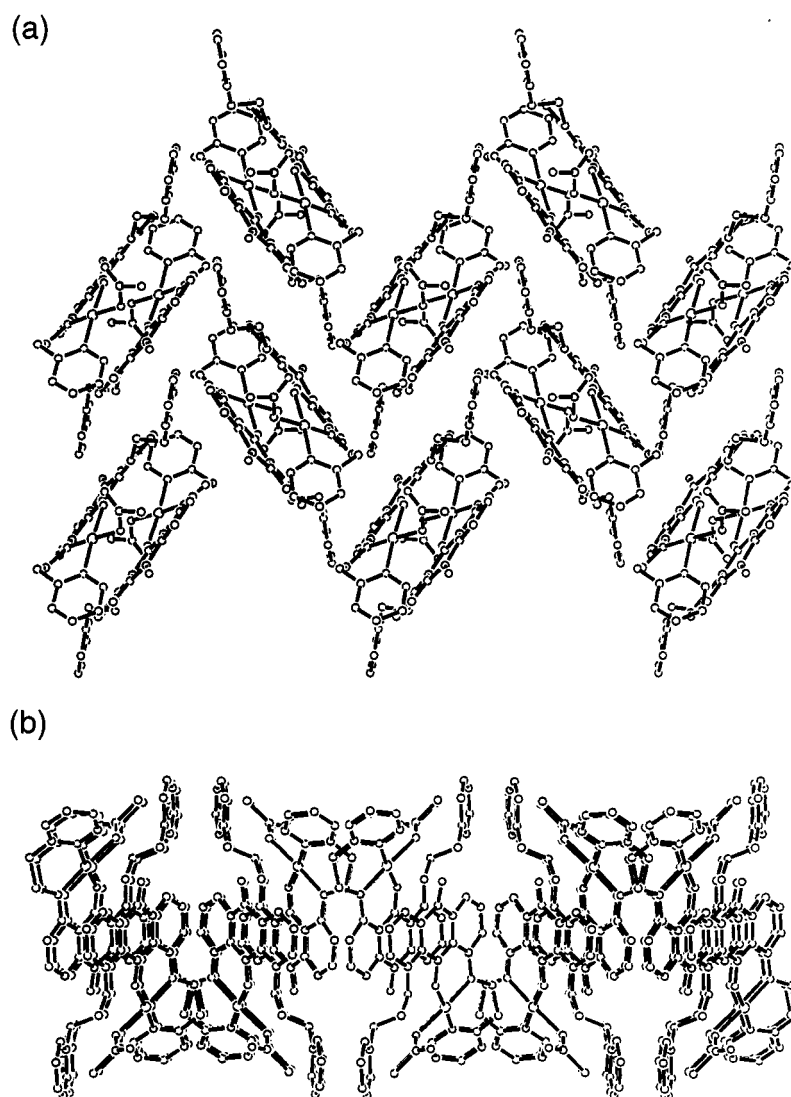


Figure 9. (a) Top view and (b) side view of the herringbone packing of the  $\pi$ -stack dimer in the crystal packing of **2b**



conformational enantiomers is low in solution. In the crystal packing (Figure 9), these enantiomers are present in a face-to-face manner with an interplanar distance of ca. 3.5 Å between the anthraquinone moieties, which form a  $\pi$ -

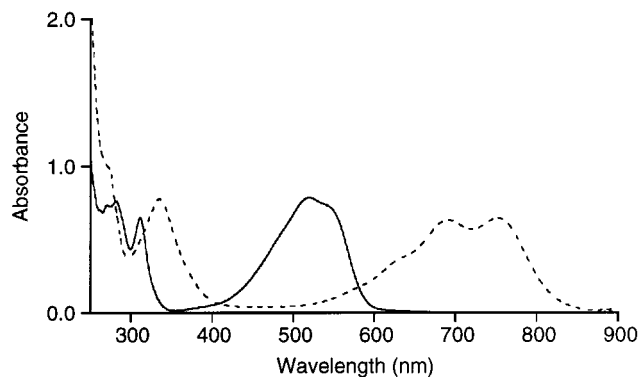


Figure 10. UV/Vis spectra of **1c** (—) ( $5.0 \times 10^{-5}$  M) and **2c** (---) ( $5.0 \times 10^{-5}$  M) in  $\text{CH}_2\text{Cl}_2$  under argon

stacked dimer that arranges in a herringbone motif with the virtues of offset stacking and edge-to-face contacts. Additionally, intramolecular hydrogen bonding between NH and C=O (quinone) [N(3)⋯O(2), 2.60 Å; H⋯O(2), 1.8 Å; N(103)⋯O(102), 2.60 Å; H⋯O(102), 1.8 Å] remains upon complexation.

Terminal bimetallic complexes with  $\pi$ -conjugated bridging spacers have recently received much attention as functional materials.<sup>[7]</sup> From this point of view, the construction of a conjugated bimetallic complex system with the 1,5-disubstituted anthraquinone ligand **1c** was examined. Treatment of **1c** with two equivalents of  $\text{Pd}(\text{OAc})_2$  in acetonitrile led to the

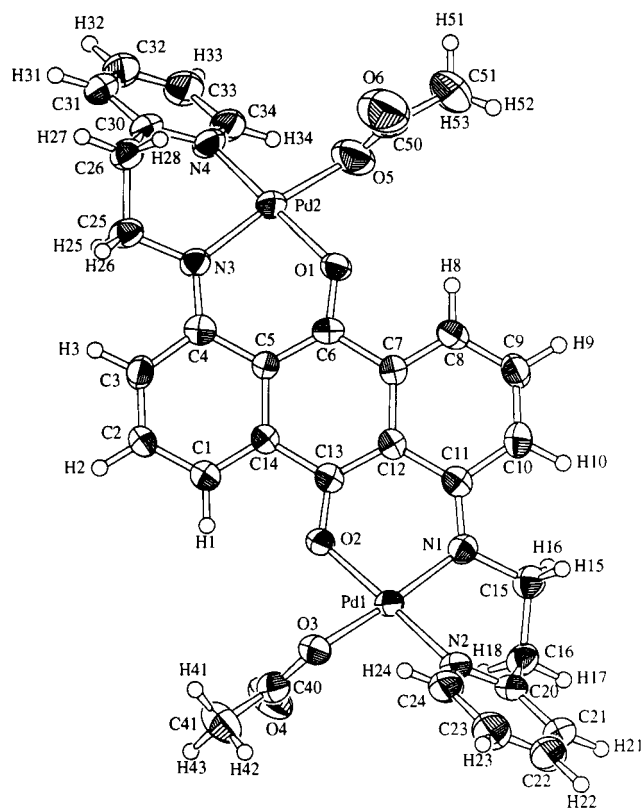


Figure 11. Molecular structure of **2c** (40% probability ellipsoids)

formation of the conjugated palladium(II) homobimetallic complex **2c** as shown in Scheme 1. Only one kind of proton signal in  $^1\text{H}$  NMR spectrum and only one C=O stretching

Table 4. Selected bond lengths [Å] and bond angles [°] for **2c**<sup>[a]</sup>

Bond lengths					
Pd(1)–O(2)	1.967(7)	1.962(7)	Pd(2)–O(1)	1.977(8)	1.960(8)
Pd(1)–O(3)	2.027(8)	2.039(8)	Pd(2)–O(5)	2.07(1)	2.034(8)
Pd(1)–N(1)	1.982(9)	1.974(9)	Pd(2)–N(3)	1.954(9)	1.969(9)
Pd(1)–N(2)	1.995(10)	2.02(1)	Pd(2)–N(4)	2.009(10)	2.010(9)
O(2)–C(13)	1.27(1)	1.27(1)	O(1)–C(6)	1.26(1)	1.26(1)
N(1)–C(11)	1.33(1)	1.33(1)	N(3)–C(4)	1.34(1)	1.36(1)
C(10)–C(11)	1.44(1)	1.43(1)	C(3)–C(4)	1.43(2)	1.43(1)
C(11)–C(12)	1.46(1)	1.45(1)	C(4)–C(5)	1.46(1)	1.45(1)
C(12)–C(13)	1.40(1)	1.42(1)	C(5)–C(6)	1.40(1)	1.39(1)
C(13)–C(14)	1.49(1)	1.48(1)	C(6)–C(7)	1.50(1)	1.48(1)
Bond angles					
O(2)–Pd(1)–O(3)	88.8(3)	85.4(3)	O(1)–Pd(2)–O(5)	88.2(4)	85.7(3)
O(2)–Pd(1)–N(1)	90.2(3)	91.4(3)	O(1)–Pd(2)–N(3)	90.0(3)	90.7(3)
O(3)–Pd(1)–N(2)	87.7(4)	90.2(4)	O(5)–Pd(2)–N(4)	88.5(4)	89.6(4)
N(1)–Pd(1)–N(2)	93.0(4)	93.0(4)	N(3)–Pd(2)–N(4)	92.5(4)	94.2(4)
O(2)–Pd(1)–N(2)	175.8(4)	173.8(4)	O(1)–Pd(2)–N(4)	174.9(4)	172.1(4)
O(3)–Pd(1)–N(1)	172.8(3)	176.8(3)	O(5)–Pd(2)–N(3)	168.9(4)	175.9(4)
C(13)–O(2)–Pd(1)	124.4(7)	128.7(7)	C(6)–O(1)–Pd(2)	124.1(7)	127.9(7)
C(11)–N(1)–Pd(1)	121.6(7)	124.4(7)	C(4)–N(3)–Pd(2)	123.8(8)	124.8(7)
O(2)–C(13)–C(14)	113.6(9)	115.1(9)	O(1)–C(6)–C(7)	114.3(9)	113.1(9)
O(2)–C(13)–C(12)	125.9(10)	124.3(10)	O(1)–C(6)–C(5)	125(1)	125.5(9)
C(11)–C(12)–C(13)	123.3(9)	123.3(9)	C(4)–C(5)–C(6)	123.1(9)	123.6(10)
C(12)–C(11)–N(1)	124.3(10)	125.1(10)	C(5)–C(4)–N(3)	123.1(10)	123.6(9)
C(10)–C(11)–N(1)	120(1)	119.9(9)	C(3)–C(4)–N(3)	120(1)	120.5(10)
C(11)–N(1)–C(15)	119.2(10)	117.1(9)	C(4)–N(3)–C(25)	116.6(9)	116.3(9)

<sup>[a]</sup> Two independent molecules exist in the asymmetric unit.

band ( $1620\text{ cm}^{-1}$ ) in the FT-IR spectrum were detected, indicating the symmetrical coordination of two quinone oxygens to each palladium. Two low-energy bands with maxima

with almost the same conformation since **2c** crystallized in the space group  $P\bar{1}$  with  $Z = 4$ . Selected bond lengths and bond angles are summarized in Table 4. Both quinone oxy-

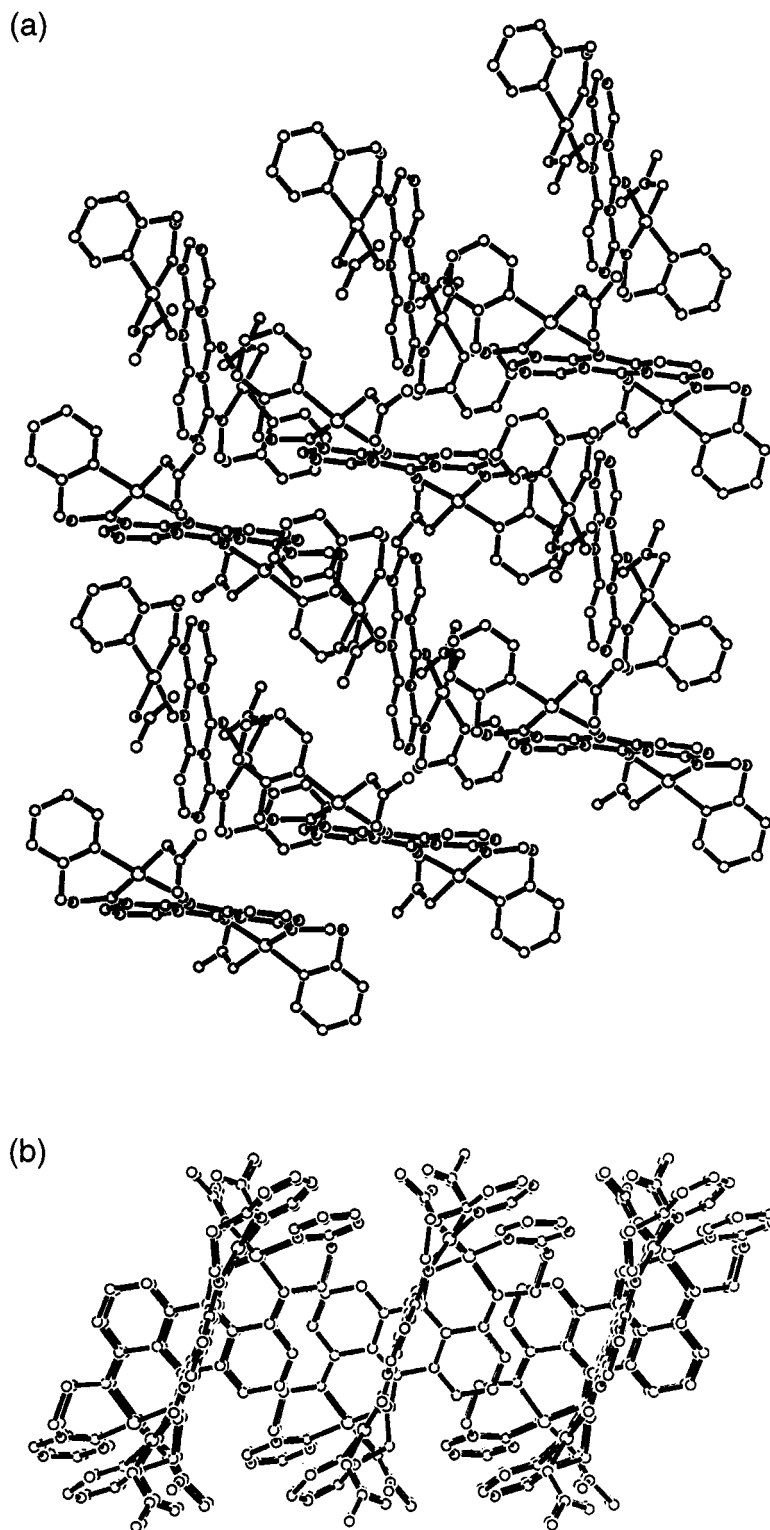


Figure 12. (a) Top view and (b) side view of the crystal packing diagram of **2c** showing edge-to-face  $\pi$ - $\pi$  interactions

around 753 and 691 nm were observed in the UV/Vis spectrum (Figure 10). The structure of **2c** was confirmed by an X-ray crystal structure determination (Figure 11 and Table 2). In the asymmetric unit, there are two independent molecules

gens participate in the coordination to each palladium. The coordination geometry around both palladium centers is almost the same. Two palladium atoms are disposed on opposite faces of the anthraquinone plane, accompanied by the



bend of quinone oxygens which lie out of the anthraquinone plane. Two palladium atoms are bridged by the quinone moiety to afford a redox-active conjugated homobimetallic complex. Two independent molecules are interconnected by an edge-to-face interaction between the anthraquinone rings in the crystal packing, as shown in Figure 12.

The redox properties of **1** and **2** were investigated by cyclic voltammetry in  $\text{CH}_2\text{Cl}_2$ . Electrochemical interest in the palladium(II) complexes in this study lies in the redox properties of the anthraquinone ligands because the complexation contributes to the electronic state. The redox potentials as listed in Table 1 are given vs. the standard  $\text{Fc}/\text{Fc}^+$  redox couple. The quinone oxygen-coordinated palladium(II) complex **2a** shows two redox couples ( $E_{1/2} = -1.73$  V and  $-1.32$  V vs.  $\text{Fc}/\text{Fc}^+$ ) assignable to stepwise one-electron reductions of the anthraquinone moiety to give the corresponding reduced species. These redox couples are positively shifted relative to the free anthraquinone ligand **1a** ( $E_{1/2} = -1.94$  V and  $-1.44$  V vs.  $\text{Fc}/\text{Fc}^+$ ) as illustrated in Figure 13. As expected, the palladium(II) homobimetallic complex **2c** exhibits a more anodic shift due to the binding of two divalent palladium. Compared with the uncomplexed one, the complexed quinone is considered to be stabilized as an electron sink.

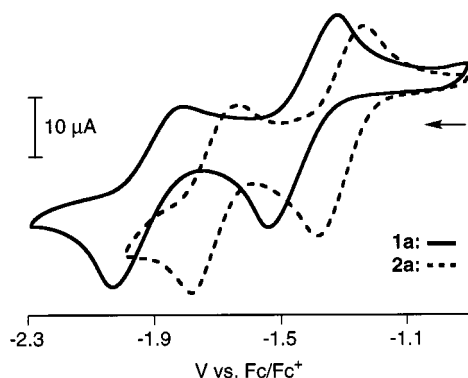


Figure 13. Cyclic voltammograms of **1a** ( $1.0 \times 10^{-3}$  M) and **2a** ( $1.0 \times 10^{-3}$  M) in  $\text{CH}_2\text{Cl}_2$  (0.1 M  $n\text{Bu}_4\text{NClO}_4$ ) at a glassy carbon working electrode with scan rate = 100 mV/s under Ar

## Conclusion

The anthraquinone ligands **1** bearing *N*-heterocyclic coordination sites have been shown to form the quinone oxygen-coordinated palladium(II) complexes. The X-ray crystal structure determination of the palladium(II) complex **2** indicates the coordination of the quinone oxygen to palladium. The conjugated palladium(II) homobimetallic complex **2c** was obtained in the case of the anthraquinone ligand bearing two *N*-heterocyclic coordination sites. The results reported in this paper reveal the aggregation properties of anthraquinone derivatives in a solid state. The anthraquinone ring plays an important role in the arrangement through the  $\pi$ - $\pi$  interactions in the crystal packing. The quinone oxygen-coordinated palladium(II) complexes **2** exhibit two redox couples based on the quinone moiety, suggesting that the complexed quinones can be considered to be stabi-

lized as an electron sink. In the palladium(II) complexes **2b–c**, the d, $\pi$ -conjugated system is revealed to interconnect through  $\pi$ - $\pi$  interactions between the  $\pi$ -conjugated systems. The controlled assembly of the redox-active conjugated complexes is envisaged to permit potential applications as functioning components of molecular devices.

## Experimental Section

**General Methods:** All reagents and solvents were purchased from commercial sources and were further purified by standard methods, if necessary. Melting points were determined on a Yanagimoto Micromelting Point apparatus and were uncorrected. Infrared spectra were obtained with a Perkin–Elmer model 1605 FT-IR.  $^1\text{H}$  NMR spectra were recorded on a Bruker AM-600 (600 MHz) or a JEOL JNM-GSX-400 (400 MHz) spectrometer with tetramethylsilane as an internal standard. Mass spectra were run on a JEOL JMS-DX303HF mass spectrometer. Electronic spectra were obtained using a Hitachi U-3000 spectrophotometer.

**Synthesis of 1-Chloro-8-[2-(2-pyridyl)ethylamino]-9,10-anthraquinone (**1a**):** A mixture of 1,8-dichloroanthraquinone (0.554 g, 2.0 mmol), 2-(2-aminoethyl)pyridine (1.22 g, 10.0 mmol), 4-dimethylaminopyridine (0.020 g, 0.16 mmol), and triethylamine (2.05 g, 20 mmol) in toluene (30 mL) was stirred under argon at reflux temperature for 7 days. After evaporation of the toluene in vacuo, the resulting mixture was dissolved in chloroform, washed with saturated  $\text{NaHCO}_3$  aqueous solution and brine, and dried over  $\text{MgSO}_4$ . The anthraquinone ligand **1a** (reddish brown needles) was isolated in 68% yield by silica-gel column chromatography and purified by recrystallization from chloroform/hexane. – M.p. 168–170 °C (uncorrected). –  $R_f = 0.45$  (ethyl acetate). – IR (KBr):  $\tilde{\nu} = 3286$  (NH), 1658 (C=O), 1635 (C=O)  $\text{cm}^{-1}$ . –  $^1\text{H}$  NMR (400 MHz,  $\text{CD}_3\text{CN}$ ):  $\delta = 3.19$  (t,  $J = 6.8$  Hz, 2 H), 3.79 (q,  $J = 6.8$  Hz, 2 H), 7.20 (ddd,  $J = 7.8, 4.9, 1.1$  Hz, 1 H), 7.28 (dd,  $J = 8.7, 1.1$  Hz, 1 H), 7.31 (ddd,  $J = 7.8, 1.1, 0.9$  Hz, 1 H), 7.46 (dd,  $J = 7.4, 1.1$  Hz, 1 H), 7.59 (dd,  $J = 8.7, 7.4$  Hz, 1 H), 7.66 (dd,  $J = 8.0, 7.7$  Hz, 1 H), 7.68 (td,  $J = 7.8, 1.9$  Hz, 1 H), 7.82 (dd,  $J = 8.0, 1.4$  Hz, 1 H), 8.18 (dd,  $J = 7.7, 1.4$  Hz, 1 H), 8.56 (ddd,  $J = 4.9, 1.9, 0.9$  Hz, 1 H), 9.60 (br, 1 H). – MS (EI):  $m/z = 362$  [ $\text{M}^+$ ]. –  $\text{C}_{21}\text{H}_{15}\text{N}_2\text{ClO}_2$  (362.81): calcd. C 69.52, H 4.17, N 7.72, Cl 9.77; found C 69.26, H 4.09, N 7.64, Cl 9.86.

**Synthesis of 1-(2-Phenylethylamino)-8-[2-(2-pyridyl)ethylamino]-9,10-anthraquinone (**1b**):** A mixture of **1a** (0.36 g, 1.0 mmol), 2-phenylethylamine (0.30 g, 2.5 mmol), 4-dimethylaminopyridine (0.010 g, 0.10 mmol), and tripropylamine (1.43 g, 10 mmol) in xylene (20 mL) was stirred under argon at reflux temperature for 7 days. After evaporation of the xylene in vacuo, the resulting mixture was dissolved in chloroform, washed with saturated  $\text{NaHCO}_3$  aqueous solution and brine, and dried over  $\text{MgSO}_4$ . The anthraquinone ligand **1b** (purple needles) was isolated in 53% yield by silica-gel column chromatography and purified by recrystallization from chloroform/hexane. – M.p. 183–184 °C (uncorrected). –  $R_f = 0.44$  (ethyl acetate/chloroform 1:1 v/v). – IR (KBr):  $\tilde{\nu} = 3263$  (NH), 1658 (C=O), 1620 (C=O)  $\text{cm}^{-1}$ . –  $^1\text{H}$  NMR (600 MHz,  $\text{CDCl}_3$ ):  $\delta = 3.08$  (t,  $J = 7.4$  Hz, 2 H), 3.24 (t,  $J = 7.1$  Hz, 2 H), 3.59 (q,  $J = 7.4$  Hz, 2 H), 3.77 (q,  $J = 7.1$  Hz, 2 H), 7.04 (d,  $J = 8.5$  Hz, 1 H), 7.10 (d,  $J = 8.5$  Hz, 1 H), 7.18 (dd,  $J = 7.6, 4.7$  Hz, 1 H), 7.26–7.29 (m, 2 H), 7.31–7.37 (m, 4 H), 7.48 (dd,  $J = 8.5, 7.6$  Hz, 2 H), 7.55 (d,  $J = 7.6$  Hz, 2 H), 7.62 (td,  $J = 7.6, 1.7$  Hz, 1 H), 8.62 (dd,  $J = 4.7, 1.7$  Hz, 1 H), 9.69 (br, 1 H), 9.73 (br, 1 H).

– MS (EI):  $m/z$  = 447 [ $M^+$ ]. –  $C_{29}H_{25}N_3O_2 \cdot 0.25H_2O$  (452.04): calcd. C 77.06, H 5.69, N 9.30; found C 77.04, H 5.57, N 9.29.

**Synthesis of 1,5-Bis[2-(2-pyridyl)ethylamino]-9,10-anthraquinone (1c):** A mixture of 1,5-dichloroanthraquinone (1.39 g, 5.0 mmol), 2-(2-aminoethyl)pyridine (3.05 g, 25 mmol), 4-dimethylaminopyridine (0.050 g, 0.40 mmol), and tripropylamine (7.16 g, 50 mmol) in toluene (70 mL) was stirred under argon at reflux temperature for 7 days. After evaporation of the toluene in vacuo, the resulting mixture was dissolved in chloroform, washed with saturated  $NaHCO_3$  aqueous solution and brine, and dried over  $MgSO_4$ . The anthraquinone ligand **1c** (red brown needles) was isolated in 12% yield by silica-gel column chromatography and purified by recrystallization from chloroform/hexane. – M.p. 169–170 °C (uncorrected). –  $R_f$  = 0.30 (ethyl acetate). – IR (KBr):  $\tilde{\nu}$  = 3255 (NH), 1620 (C=O)  $cm^{-1}$ . –  $^1H$  NMR (400 MHz,  $CD_3CN$ ):  $\delta$  = 3.17 (t,  $J$  = 6.9 Hz, 4 H), 3.76 (q,  $J$  = 6.9 Hz, 4 H), 7.15 (dd,  $J$  = 8.5, 1.0 Hz, 2 H), 7.21 (ddd,  $J$  = 7.7, 4.9, 1.0 Hz, 2 H), 7.32 (ddd,  $J$  = 7.7, 1.0, 0.8 Hz, 2 H), 7.45 (dd,  $J$  = 7.5, 1.0 Hz, 2 H), 7.55 (dd,  $J$  = 8.5, 7.5 Hz, 2 H), 7.69 (td,  $J$  = 7.7, 1.9 Hz, 2 H), 8.54 (ddd,  $J$  = 4.9, 1.9, 0.8 Hz, 2 H), 9.70 (br, 2 H). – MS (EI):  $m/z$  = 448 ( $M^+$ ). –  $C_{28}H_{24}N_4O_2 \cdot 0.5H_2O$  (457.53): calcd. C 73.51, H 5.51, N 12.25; found C 73.29, H 5.33, N 12.15.

**General Procedure for the Preparation of the Palladium(II) Complex 2:** To anthraquinone ligand **1** (0.20 mmol) in acetonitrile (40 mL) was added an acetonitrile solution (10 mL) of  $Pd(OAc)_2$  (44.9 mg, 0.20 mmol) under argon. For the preparation of **2c**, two equiv. of  $Pd(OAc)_2$  were used. Stirring at room temperature for 5 h in the dark afforded a blue solution. After evaporation of the solvent in vacuo, the palladium(II) complex **2** was quantitatively isolated by recrystallization from acetonitrile.

**2a:** M.p. 235–236 °C (decomp.). – IR (KBr):  $\tilde{\nu}$  = 1651 (C=O), 1620 (C=O)  $cm^{-1}$ . –  $^1H$  NMR (400 MHz,  $CD_3CN$ ):  $\delta$  = 1.85 (s, 3 H), 3.26–3.30 (m, 2 H), 3.55–3.58 (m, 2 H), 7.27 (dd,  $J$  = 8.8, 1.8 Hz, 1 H), 7.30–7.36 (m, 3 H), 7.53 (d,  $J$  = 7.7 Hz, 1 H), 7.63 (dd,  $J$  = 8.0, 7.8 Hz, 1 H), 7.79 (dd,  $J$  = 8.0, 1.4 Hz, 1 H), 7.93 (td,  $J$  = 7.7, 1.6 Hz, 1 H), 8.14 (dd,  $J$  = 7.8, 1.4 Hz, 1 H), 8.49 (dd,  $J$  = 5.8, 1.6 Hz, 1 H). – MS (FAB):  $m/z$  = 469 [ $M - OAc + 1$ ] $^+$ . –  $C_{23}H_{17}ClN_2O_4Pd \cdot H_2O$  (545.29): calcd. C 50.66, H 3.51, N 5.14, Cl 6.50; found C 50.74, H 3.51, N 5.38, Cl 6.55.

**2b:** M.p. 244–245 °C (decomp.). – IR (KBr):  $\tilde{\nu}$  = 1643 (C=O), 1620 (C=O)  $cm^{-1}$ . –  $^1H$  NMR (400 MHz,  $CD_2Cl_2$ ):  $\delta$  = 1.87 (s, 3 H), 2.94–2.98 (m, 2 H), 3.14–3.16 (m, 2 H), 3.51–3.56 (m, 4 H), 7.03–7.06 (m, 1 H), 7.08 (dd,  $J$  = 9.1, 1.1 Hz, 1 H), 7.20–7.31 (m, 7 H), 7.32 (dd,  $J$  = 6.9, 1.1 Hz, 1 H), 7.41 (ddd,  $J$  = 7.6, 1.4, 0.8 Hz, 1 H), 7.43–7.45 (m, 2 H), 7.83 (td,  $J$  = 7.6, 1.5 Hz, 1 H), 8.58 (ddd,  $J$  = 5.9, 1.5, 0.8 Hz, 1 H), 8.73 (br, 1 H). – MS (FAB)  $m/z$  = 553 [ $M - OAc + 1$ ] $^+$ . –  $C_{31}H_{27}N_3O_4Pd \cdot 0.5H_2O$  (621.0): calcd. C 59.96, H 4.54, N 6.77; found C 60.07, H 4.49, N 7.07.

**2c:** M.p. 245–246 °C (decomp.). – IR (KBr):  $\tilde{\nu}$  = 1620 (C=O)  $cm^{-1}$ . –  $^1H$  NMR (600 MHz,  $CD_2Cl_2$ ):  $\delta$  = 1.86 (s, 6 H), 3.11–3.13 (m, 4 H), 3.43–3.46 (m, 4 H), 6.91 (d,  $J$  = 9.2 Hz, 2 H), 7.12 (dd,  $J$  = 9.2, 7.0 Hz, 2 H), 7.14 (ddd,  $J$  = 7.6, 5.6, 1.2 Hz, 2 H), 7.25 (d,  $J$  = 7.0 Hz, 2 H), 7.29 (dd,  $J$  = 7.6, 1.2 Hz, 2 H), 7.72 (td,  $J$  = 7.6, 1.4 Hz, 2 H), 8.47 (dd,  $J$  = 5.6, 1.4 Hz, 2 H). – MS (FAB):  $m/z$  = 660 [ $M - 2 OAc + 1$ ] $^+$ . –  $C_{32}H_{28}N_4O_6Pd_2 \cdot CH_3CN$  (818.49): calcd. C 49.89, H 3.82, N 8.56; found C 49.25, H 3.61, N 8.95.

**Electrochemical Experiments:** The cyclic voltammetry measurements were performed on a BAS CV-50 W voltammetry analyzer in deaerated  $CH_2Cl_2$ , containing 0.1 M  $nBu_4NClO_4$  as a supporting

electrolyte, at 298 K, with a three-electrode system consisting of a highly polished glassy carbon working electrode (BAS), a platinum auxiliary electrode (BAS), and an Ag/AgCl (0.01 M) reference electrode (BAS), at 100 mV/s scan rate. Potentials are given vs.  $Fc/Fc^+$  as an internal standard.

**X-ray Crystal Structure Determination:** All measurements for **1a**, **2a**, **2b**, and **2c** were made on a Rigaku AFC5R diffractometer with graphite monochromated Mo- $K_\alpha$  radiation and a rotating anode generator. The structures of **1a**, **2a**, and **2b** were solved by direct methods and expanded using Fourier techniques. The structure of **2c** was solved by heavy-atom Patterson methods and expanded using Fourier techniques. The non-hydrogen atoms were refined anisotropically. The H atoms involved in hydrogen bonding were located in electron density maps. The remainder of the H atoms were placed in idealized positions and allowed to ride with the C atoms to which each is bonded. Crystallographic details are given in Table 2. Crystallographic data (excluding structure factors) for the structures reported in this paper have been deposited with the Cambridge Crystallographic Data Centre as supplementary publication no. CCDC-146561 for **1a**, -146562 for **2a**, -146563 for **2b**, and -146564 for **2c**. Copies of the data can be obtained free of charge on application to CCDC, 12 Union Road, Cambridge CB2 1EZ, UK [Fax: (internat.) +44-1223/336-033; E-mail: deposit@ccdc.cam.ac.uk].

## Acknowledgments

This work was financially supported in part by a Grant-in-Aid for Scientific Research on Priority Areas from the Ministry of Education, Science, and Culture, Japan. Thanks are also due to the Analytical Center, Faculty of Engineering, Osaka University for the use of their facilities.

- [1] [1a] C. G. Pierpont, H. H. Downs, T. G. Rukavina, *J. Am. Chem. Soc.* **1974**, *96*, 5573. – [1b] R. M. Buchanan, S. L. Kessel, H. H. Downs, C. G. Pierpont, D. N. Hendrickson, *J. Am. Chem. Soc.* **1978**, *100*, 7894. – [1c] S. R. Sofen, D. C. Ware, S. R. Cooper, K. N. Raymond, *Inorg. Chem.* **1979**, *18*, 234. – [1d] C. G. Pierpont, R. M. Buchanan, *Coord. Chem. Rev.* **1981**, *38*, 45. – [1e] M. E. Cass, D. L. Greene, R. M. Buchanan, C. G. Pierpont, *J. Am. Chem. Soc.* **1983**, *105*, 2680. – [1f] M. W. Lynch, D. N. Hendrickson, B. J. Fitzgerald, C. G. Pierpont, *J. Am. Chem. Soc.* **1984**, *106*, 2041. – [1g] M. Haga, E. S. Dodsworth, A. B. P. Lever, *Inorg. Chem.* **1986**, *25*, 447. – [1h] H. Masui, A. B. P. Lever, P. R. Auburn, *Inorg. Chem.* **1991**, *30*, 2402. – [1i] D. M. Adams, A. Dei, A. L. Rheingold, D. N. Hendrickson, *Angew. Chem. Int. Ed. Engl.* **1993**, *32*, 880. – [1j] L. F. Joulie, E. Schatz, M. D. Ward, F. Weber, L. J. Yellowlees, *J. Chem. Soc., Dalton Trans.* **1994**, 799. – [1k] C. G. Pierpont, C. W. Lange, *Prog. Inorg. Chem.* **1994**, *41*, 331. – [1l] A. M. Barthram, R. L. Cleary, R. Kowallick, M. D. Ward, *Chem. Commun.* **1998**, 2695.
- [2] [2a] J. E. Bäckvall, S. E. Byström, R. E. Nordberg, *J. Org. Chem.* **1984**, *49*, 4619. – [2b] J. E. Bäckvall, A. Gogoll, *Tetrahedron Lett.* **1988**, *29*, 2243. – [2c] J. E. Bäckvall, R. B. Hopkins, H. Grennberg, M. M. Mader, A. K. Awasthi, *J. Am. Chem. Soc.* **1990**, *112*, 5160. – [2d] A. Thorarensen, A. Palmgren, K. Itami, J. E. Bäckvall, *Tetrahedron Lett.* **1997**, *38*, 8541. – [2e] K. Bergstad, H. Grennberg, J. E. Bäckvall, *Organometallics* **1998**, *17*, 45.
- [3] [3a] M. Hiramatsu, H. Nakano, T. Fujinami, S. Sakai, *J. Organomet. Chem.* **1982**, *236*, 131. – [3b] M. Hiramatsu, K. Shiozaki, T. Fujinami, S. Sakai, *J. Organomet. Chem.* **1983**, *246*, 203. – [3c] R. A. Klein, C. J. Elsevier, F. Hartl, *Organometallics* **1997**, *16*, 1284.
- [4] [4a] S. S. Massoud, R. B. Jordan, *Inorg. Chem.* **1991**, *30*, 4851. – [4b] A. DelMedico, P. R. Auburn, E. S. Dodsworth, A. B. P. Lever, W. J. Pietro, *Inorg. Chem.* **1994**, *33*, 1583.
- [5] T. Moriuchi, S. Bandoh, M. Miyaishi, T. Hirao, *Eur. J. Inorg. Chem.* in press.

- [6] [6a] C. J. da Cunha, S. S. Fielder, D. V. Stynes, H. Masui, P. R. Auburn, A. B. P. Lever, *Inorg. Chim. Acta* **1996**, *242*, 293. — [6b] K. Ochiai, Y. Mazaki, S. Nishikiori, K. Kobayashi, S. Hayashi, *J. Chem. Soc., Perkin Trans. 2* **1996**, 1139. — [6c] B. S. Joshi, T. Rho, P. L. Rinaldi, W. Liu, T. A. Wagler, M. G. Newton, D. Lee, S. W. Pelletier, *J. Chem. Crystallogr.* **1997**, *27*, 553.
- [7] [7a] M. Haga, T. Ano, K. Kano, S. Yamabe, *Inorg. Chem.* **1991**, *30*, 3843. — [7b] J.-P. Sauvage, J.-P. Collin, J.-C. Chambron, S. Guillerez, C. Coudret, V. Balzani, F. Barigelletti, L. De Cola, L. Flamigni, *Chem. Rev.* **1994**, *94*, 993. — [7c] W. Weng, T. Bartik, J. A. Gladysz, *Angew. Chem. Int. Ed. Engl.* **1994**, *33*, 2199. — [7d] M. D. Ward, *Chem. Soc. Rev.* **1995**, 121. — [7e] N. Le Narvor, L. Toupet, C. Lapinte, *J. Am. Chem. Soc.* **1995**, *117*, 7129. — [7f] A. Harriman, R. Ziessel, *Chem. Commun.* **1996**, 1707. — [7g] O. Lavastre, J. Plass, P. Bachmann, S. Guesmi, C. Moinet, P. H. Dixneuf, *Organometallics* **1997**, *16*, 184. — [7h] N. D. Jones, M. O. Wolf, D. M. Giaquinta, *Organometallics* **1997**, *16*, 1352. — [7i] M. M. Richter, A. J. Bard, W. Kim, R. H. Schmehl, *Anal. Chem.* **1998**, *70*, 310. — [7j] J. A. McCleverty, M. D. Ward, *Acc. Chem. Res.* **1998**, *31*, 842. — [7k] M. Hissler, A. El-ghayoury, A. Harriman, R. Ziessel, *Angew. Chem. Int. Ed.* **1998**, *37*, 1717. — [7l] T. Bartik, W. Weng, J. A. Ramsden, S. Szafert, S. B. Falloon, A. M. Arif, J. A. Gladysz, *J. Am. Chem. Soc.* **1998**, *120*, 11071. — [7m] E. C. Constable, C. E. Housecroft, E. R. Schofield, S. Encinas, N. Armaroli, F. Barigelletti, L. Flamigni, E. Figgemeier, J. G. Vos, *Chem. Commun.* **1999**, 869.

Received July 3, 2000  
[100264]